

Driven Morse oscillator: Classical chaos, quantum theory, and photodissociation

M. E. Goggin and P. W. Milonni

Theoretical Division, Los Alamos National Laboratory, Los Alamos, New Mexico 87545

(Received 20 July 1987)

We compare the classical and quantum theories of a Morse oscillator driven by a sinusoidal field, focusing attention on multiple-photon excitation and dissociation. In both the classical and quantum theories the threshold field strength for dissociation may be estimated fairly accurately on the basis of classical resonance overlap, and the classical and quantum results for the threshold are in good agreement except near higher-order classical resonances and quantum multiphoton resonances. We discuss the possibility of "quantum chaos" in such driven molecular systems and use the Morse oscillator to test the manifestations of classical resonance overlap suggested semi-classically.

I. INTRODUCTION

For over half a century the Morse potential has provided a useful basis for interpreting and fitting the vibrational spectra of diatomic molecules.¹ In the last few years the *classical* Morse oscillator driven by a sinusoidal force has been invoked in studies of stochastic excitation and dissociation associated with the onset of chaos. Davis and Wyatt, for instance, find that dissociation always occurs from what would appear to be chaotic regions of phase space in the classical model.² Galvao *et al.* have made estimates of the classical threshold for stochastic excitation and dissociation based on Chirikov's resonance overlap criterion.^{3,4} They find, based on numerical integration of classical trajectories, that the dissociation rate scales approximately with the laser intensity, in agreement with the earlier studies of Shuryak.⁵

A number of classical studies have pointed to the importance of chaos in the infrared multiple-photon excitation and dissociation of molecules.⁶ In particular, the chaotic meandering of trajectories in phase space can result in a diffusive energy growth in which the average energy grows linearly with time, leading eventually to dissociation. On the other hand, it is known from models like the periodically kicked pendulum that quantum effects can suppress this diffusive behavior and produce a phase-space localization analogous to the Anderson localization of a particle moving on a lattice with random site energies.⁷ The question therefore arises as to the range of validity of the rather large number of classical models.

This question, of course, is an old one, and the answer depends on what one is trying to accomplish with a classical model. In the context of molecular excitation and dissociation, classical models have long been advocated on intuitive grounds,⁸ but only rarely have classical and quantum models been directly compared. An important exception is the work of Walker and Preston,⁹ in which classical and quantum results for a sinusoidally driven Morse oscillator were compared. Using parameters ap-

propriate to the HF (hydrogen fluoride) molecule, these authors found that gross features of quantities like the expectation value of energy or position, as functions of time, could be fairly well predicted by averaging over classical trajectories. Multiphoton resonances, however, were not well accounted for by the classical theory.

Another reason for making detailed comparisons of classical and quantum computations is to better understand the quantum-mechanical manifestations of classical chaos. That is, how does the onset of classical chaos manifest itself when the system is treated fully quantum mechanically? This question of "quantum chaos" has been a difficult and controversial one; some aspects of it are discussed in this paper. Our main goal here is to extend the work of Walker and Preston to include the possibility of dissociation. We do this by direct numerical solution of the time-dependent, Schrödinger partial differential equation. This approach may be extended to include molecular rotations, and we plan to discuss this extension in a future publication.

Section II summarizes the classical model and addresses the question of resonance overlap. In Sec. III we present some results of the classical model and discuss the onset and rate of photodissociation. Section IV summarizes our approach to the numerical solution of the time-dependent Schrödinger equation, and we consider a simple quantum-mechanical extension of the notion of resonance overlap. In Sec. V we discuss the quantum-mechanical results for multiple-photon excitation and dissociation of the Morse oscillator, and compare these results with the corresponding classical trajectory theory. In Sec. VI we take up questions of chaos and summarize our conclusions from this work.

II. CLASSICAL DRIVEN MORSE OSCILLATOR

We consider the time-dependent Hamiltonian

$$H = p^2/2m + D(1 - e^{-ax})^2 - d_1 E_0 x \cos(\omega_L t) \quad (2.1)$$

and integrate the classical equations of motion

$$\dot{x} = p/m, \quad (2.2a)$$

$$\dot{p} = -2Da(e^{-ax} - e^{-2ax}) + d_1 E_0 \cos(\omega_L t), \quad (2.2b)$$

where D and a are the dissociation energy and range parameter, respectively, of the Morse potential, and d_1 is the effective charge, or dipole gradient. Near the bottom of the well we have approximately harmonic motion with frequency $\omega_0 = (2Da^2/m)^{1/2}$.

For $E_0 = 0$ the motion is, of course, integrable. The action variable is

$$\begin{aligned} J &= (1/2\pi) \oint p \, dq = (1/\pi) \int_{x_1}^{x_2} p \, dq \\ &= (1/\pi) \sqrt{2m} \int_{x_1}^{x_2} dx \sqrt{E - V(x)}, \end{aligned} \quad (2.3)$$

where x_1, x_2 are the turning points [$V(x_i) = E, i = 1, 2$]. For the Morse potential we obtain $J = -(2m/a^2)^{1/2}(\sqrt{D-E} - \sqrt{D})$ and therefore the unperturbed energy and frequency as functions of the action J are

$$E = \omega_0(J - \omega_0 J^2/4D), \quad (2.4a)$$

$$\dot{\theta} = \omega(J) = \partial E / \partial J = \omega_0(1 - \omega_0 J/2D), \quad (2.4b)$$

as, of course, is well known. We may write $x(t)$ in terms of the angle variable θ as follows:

$$x(J, \theta) = a^{-1} \ln \left[\frac{D + \sqrt{DE} \cos \theta}{D - E} \right], \quad (2.5)$$

where the values $\theta = 0$ and π correspond to the outer and inner turning points, respectively, of the unperturbed motion.

To investigate qualitatively the behavior of the driven Morse oscillator ($E_0 \neq 0$), we consider Chirikov's resonance overlap criterion. For this purpose, the Hamiltonian (2.1) is expressed in terms of the action-angle variables θ, J as follows:

$$\begin{aligned} H &= H_0(J) - (d_1 E_0/a) \ln \left[\frac{D + \sqrt{DE} \cos \theta}{D - E} \right] \cos(\omega_L t) \\ &= H_0(J) - 2 \sum_{N=0}^{\infty} V_N(J) \cos(N\theta) \cos(\omega_L t) \\ &= H_0(J) - \sum_{N=0}^{\infty} V_N(J) [\cos(N\theta + \omega_L t) \\ &\quad + \cos(N\theta - \omega_L t)], \end{aligned} \quad (2.6)$$

where

$$V_N(J) = (d_1 E_0/2\pi) \int_0^{2\pi} d\theta x(J, \theta) \cos(N\theta) \quad (2.7)$$

and $H_0(J) = \omega_0(J - \omega_0 J^2/4D)$. Near an isolated resonance defined by

$$\omega_L = N\dot{\theta} = N\omega(J_N) \quad (2.8)$$

we make a "rotating-wave approximation" in which only the most slowly varying part of the perturbation is retained in (2.6),

$$H \rightarrow H_{\text{RWA}} = H_0(J) - V_N(J) \cos(N\theta - \omega_L t). \quad (2.9)$$

Following Chirikov's line of reasoning⁴ we write

$$J = J_N + NP \quad (2.10)$$

and assume P is small enough that $V_N(J) \cong V_N(J_N)$. We also define

$$Q = \omega_L t - N\theta \quad (2.11)$$

so that

$$\dot{P} = N^{-1} \dot{J} = -N^{-1} \frac{\partial H_{\text{RWA}}}{\partial \theta} = V_N(J_N) \sin Q, \quad (2.12a)$$

$$\begin{aligned} \dot{Q} &= \omega_L - N\dot{\theta} \\ &= -N\omega_0 + (N\omega_0^2/2D)(J_N + NP) + \omega_L \\ &= (N^2\omega_0^2/2D)P \\ &\equiv P/M_N. \end{aligned} \quad (2.12b)$$

Thus Q and P are coordinate and momentum variables for the pendulum system with Hamiltonian

$$H = P^2/2M_N + V_N(J_N) \cos Q, \quad M_N \equiv 2D/N^2\omega_0^2. \quad (2.13)$$

From (2.5) and (2.7) we have

$$\begin{aligned} V_N(J) &= (d_1 E_0/a) A_N, \\ A_N &\equiv (-1)^{N+1}/N [\sqrt{D/E} (1 + \sqrt{1 - E/D})]^{-N} \\ &= (-1)^{N+1}/N \left[\frac{1 - \omega_L/N\omega_0}{1 + \omega_L/N\omega_0} \right]^{N/2}, \quad N \neq 0. \end{aligned} \quad (2.14)$$

Here ω_L is the laser frequency at which the resonance condition (2.8) is satisfied,

$$\omega_L = N\omega_0 \sqrt{1 - E/D}. \quad (2.15)$$

We are now in a position to formulate Chirikov's resonance overlap criterion for the driven Morse oscillator. According to this criterion, the onset of chaos is expected roughly when the sum of the widths of neighboring resonance zones exceeds the distance between the zones in action-angle space. The width of the N th resonance may be inferred from (2.13): the maximum excursion of P for the pendulum system (2.13) is $\Delta P = \sqrt{2M_N |V_N(J_N)|}$ so that, from (2.10),

$$\Delta J_N = N \sqrt{2M_N |V_N(J_N)|} = 2\sqrt{D}/\omega_0 \sqrt{|V_N(J_N)|} \quad (2.16)$$

is the width in the action variable associated with resonance N . The resonance overlap criterion for the onset of chaos then takes the form

$$\Delta J_{N+1} + \Delta J_N > J_{N+1} - J_N \quad (2.17)$$

or, using (2.8), (2.14), and (2.15),

$$d_1 E_0 / Da > (\omega_L / \omega_0)^2 N^{-2} (N+1)^{-2} \times (|A_{N+1}|^{1/2} + |A_N|^{1/2})^{-2}. \quad (2.18)$$

This is equivalent to the condition $\Delta\omega_{N+1} + \Delta\omega_N > \omega_{N+1} - \omega_N$, where ω_N is the resonance frequency satisfying (2.8) and $\Delta\omega_N$ is the spread in this frequency associated with the width of the action variable.

Consider, for instance, the classical Morse oscillator with energy corresponding to the ground state of the quantum system,

$$E \cong BD = 0.0419D, \quad (2.19)$$

where the value of B is chosen to correspond to the Morse parameters for the HF molecule, for which $D = 6.125$ eV (Sec. IV). Then for an $N=1$ resonance $\omega_L = 0.979\omega_0$ and we calculate $A_1 = 0.10$, $A_2 = -0.17$, and the resonance overlap condition $d_1 E_0 / Da > 0.45$ or

$$K \equiv d_1 E_0 / DB^2 a > 256. \quad (2.20)$$

It must be emphasized that the resonance overlap condition (2.18) provides only a rough estimate of the field strength at which chaos might be anticipated. We will see in Sec. III that in fact the estimate (2.20) is more than a factor of 2 larger than the value of K necessary for dissociation. It is perhaps worth noting that (2.18) has a simpler form than the resonance overlap criterion derived by Galvao *et al.*³

III. CLASSICAL COMPUTATIONS

Since we wish to compare with the quantum theory of the driven Morse oscillator, we average the classical results over a large number of trajectories with different initial conditions. This is done by fixing the energy E of the initially unperturbed oscillator, setting the momentum $p = \pm\sqrt{2m[E - V(x)]}$, and sampling the x values according to a uniform distribution on the interval be-

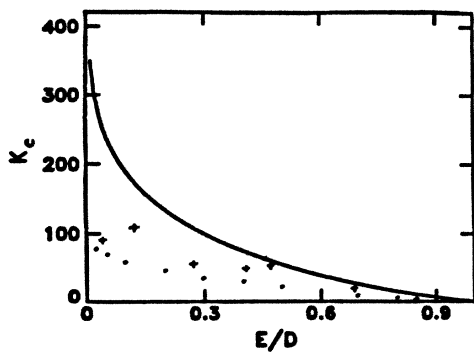


FIG. 1. The critical pump parameter K_c for dissociation vs E/D , determined from the resonance overlap condition (2.18) (—), classical trajectory analysis (\bullet), and the Schrödinger equation ($+$). For each E/D the laser frequency is set to the classical nonlinear resonance value (2.15) with $N=1$. The Morse parameters are those appropriate to HF.

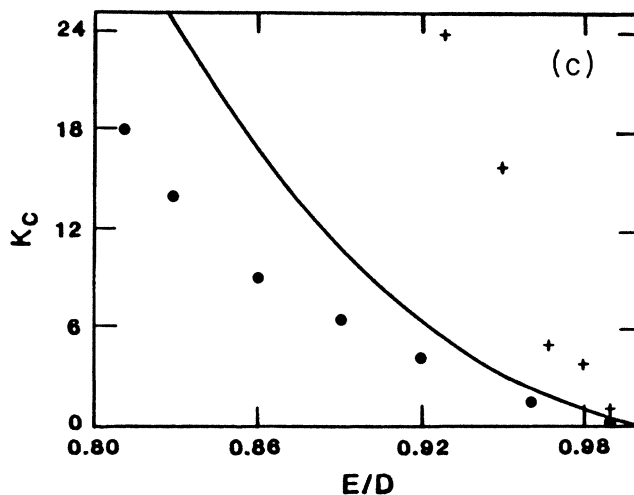
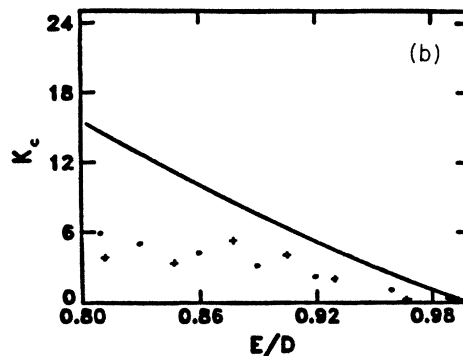
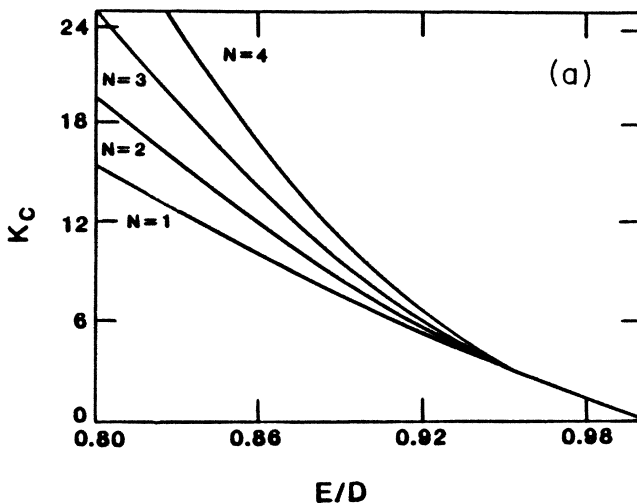


FIG. 2. (a) K_c vs E/D given by the resonance overlap condition (2.18) as in Fig. 1 for $N=1, 2, 3$, and 4 resonances; (b) K_c as in (a) for $N=1$, together with the classical (\bullet) and quantum ($+$) predictions; (c) as in (b) for an $N=4$ nonlinear resonance.

tween the two classical turning points. [We have also performed computations in which the x 's are distributed according to the quantum-mechanical probability density $|\psi(x)|^2$ for a stationary state of energy E , but the results were very similar to those with a uniform x distribution.] To further facilitate the comparison of the classical and quantum theories, we generally choose E to correspond to an energy eigenvalue of the quantum-mechanical Morse oscillator (Sec. IV).

Some aspects of the classical and quantum results are summarized in Sec. V. In this section we focus our attention on some classical predictions for the photodissociation of the Morse oscillator. For this purpose we consider the "compensated energy"¹⁰

$$E_c = \left[m\dot{x} - \frac{d_1 E_0}{\omega} \sin(\omega t) \right]^2 / 2m + V(x), \quad (3.1)$$

which is constant when $V(x) \equiv 0$. As such, the compensated energy varies more smoothly than the energy $\frac{1}{2}m\dot{x}^2 + V(x)$. Following the work of Leopold and Percival¹⁰ on an analogous ionization problem, we define dissociation in our computations by the condition $E_c > D$. The dissociation probability is defined as the fraction of sampled trajectories for which $E_c > D$.

Equation (2.18) provides an estimate of the critical pump parameter K_c necessary for resonance overlap. We plot this K_c versus E/D in Fig. 1 for the case of an $N=1$ resonance, and compare with the corresponding critical pump parameters for dissociation determined from the classical trajectory calculations. (For the Morse parameters of HF the field intensity I may be obtained from $K = d_1 E_0 / DB^2 a$ by the relation $I = 0.08K^2$ TW/cm².) In the trajectory computations K_c was defined as the value of K , for fixed E/D , that causes dissociation of $\approx 1-3$ trajectories out of 500 within 90 optical cycles. This value of K_c was typically two or three

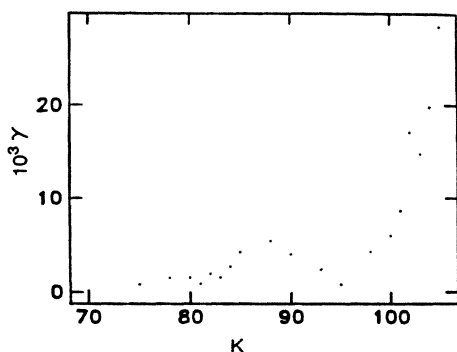


FIG. 3. The classically predicted dissociation rate γ (per optical cycle) as a function of K for an initial energy equal numerically to the quantum ground-state energy for the Morse oscillator. The field frequency is slightly redshifted from the resonant value for the quantum $n=0 \rightarrow n=1$ transition, and is close to the value for an $N=1$ resonance.

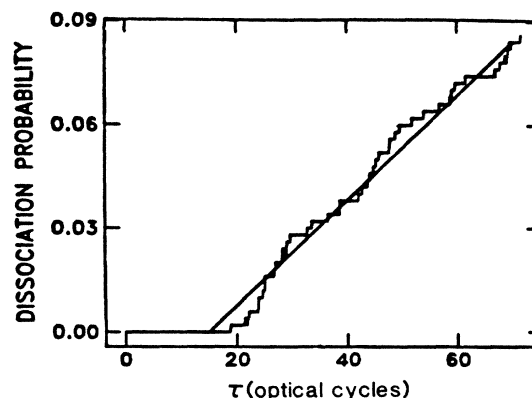


FIG. 4. The classical dissociation rate is defined by fitting a straight line to the curve of dissociation probability vs time, as indicated. In this case we chose $K=80$ and $\mu=45.11$ and the molecule was initially in the ground state.

times smaller than the value predicted by the simple resonance overlap criterion derived above. However, the curves of K_c versus E/D are seen in Fig. 1 to be qualitatively similar. This can also be seen in Fig. 2, where we plot K_c versus E/D for the $N=1, 2, 3$, and 4 resonances.

Figure 3 shows the dissociation rate γ as a function of K for an initial energy equal numerically to the quantum-mechanical ground-state energy; the driving frequency is chosen to be slightly redshifted from the $n=0 \rightarrow n=1$ transition of the quantum system, and corresponds closely to an $N=1$ resonance in the classical system. The dissociation rate was defined by fitting a straight line to a plot of the dissociation probability versus time, as illustrated in Fig. 4. For strong fields the dissociation probability as a function of time has a saturation behavior, as illustrated in Fig. 5 after ≈ 30 cycles. In such cases the dissociation rate is defined by the short-term, nonsaturated part of the curve.

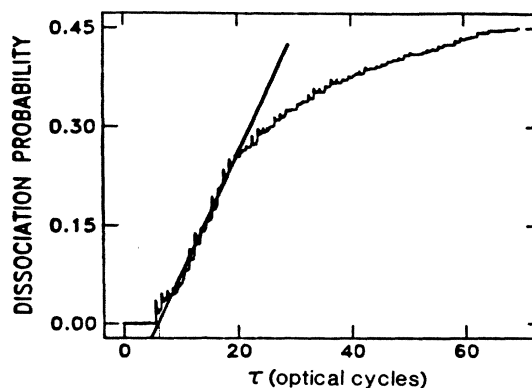


FIG. 5. For large values of the dissociation probability there is a saturation of the dissociation probability because fewer and fewer trajectories are available for dissociation. In this case, $K=160$.

IV. QUANTUM SYSTEM

The eigenfunctions for the unperturbed Morse oscillator are¹¹

$$\psi_n(x) = A_n e^{-z/2} z^{[(k-1)-2n]/2} L_{k-n}^{k-2n}(z), \quad n=0,1,2,\dots, \quad (4.1)$$

where A_n is a normalization constant, L_n^m is the generalized Laguerre polynomial, and

$$z = ke^{-ax}, \quad (4.2a)$$

$$k = 4D/\hbar\omega_0, \quad (4.2b)$$

$$\omega_0 = (2Da^2/m)^{1/2}. \quad (4.2c)$$

The corresponding energy eigenvalues are given very accurately by^{9,11}

$$E_n = BD(n + \frac{1}{2})[2 - B(n + \frac{1}{2})], \quad (4.3)$$

where

$$B = (\hbar^2 a^2 / 2mD)^{1/2}. \quad (4.4)$$

The Morse parameters for HF are taken from Walker and Preston:⁹ $B = 0.0419$, $D = 6.125$ eV, $a = 1.1741a_0^{-1}$, and $d_1 = 0.7876 D/a_0$. For these parameters the Morse potential allows 24 bound states.

In order to compare with the classical theory described in Sec. III, we solve the time-dependent Schrödinger equation

$$i\hbar \frac{\partial \psi}{\partial t} = \left[-\frac{\hbar^2}{2m} \frac{\partial^2}{\partial x^2} + D(1 - e^{-ax})^2 - d_1 E_0 \cos(\omega_L t) \right] \psi. \quad (4.5)$$

Our approach is to solve this parabolic partial differential equation numerically rather than to employ a basis-state expansion for ψ and then solve the coupled ordinary differential equations for the state amplitudes. By automatically accounting for the continuum, this approach facilitates the treatment of photodissociation in our model system.

Our numerical approach involves a simple spatial discretization together with the algorithm

$$\psi_j^{n+1} = \left[\frac{1 - iH\Delta t/2\hbar}{1 + iH\Delta t/2\hbar} \right] \psi_j^n \quad (4.6)$$

for (unitary) time evolution by a step Δt . This procedure leads to a tridiagonal linear system of equations that may be solved by a well-known, efficient "two-sweep" method.¹²

In all our calculations we have written (2.2) in the scaled form

$$\frac{d^2 X}{d\tau^2} = -(4/B^2)(e^{-X} - e^{-2X}) + 2K \cos(\mu\tau), \quad (4.7)$$

where

$$\tau = (DB^2/\hbar)t, \quad (4.8a)$$

$$X = ax, \quad (4.8b)$$

$$\mu = \hbar\omega_L/DB^2, \quad (4.8c)$$

$$K = d_1 E_0 / aDB^2. \quad (4.8d)$$

In terms of these variables the Schrödinger equation takes the form

$$i \frac{\partial \psi}{\partial \tau} = -\frac{\partial^2 \psi}{\partial X^2} + B^{-2}(1 - e^{-X})\psi - KX \cos(\mu\tau)\psi. \quad (4.9)$$

One way to check our computer program for solving (4.9) is to compare with conventional basis-state approaches when the driving field is sufficiently weak that dissociation is negligible. In particular, we have compared with results shown in the paper by Walker and Preston.⁹ Figure 6, for instance, shows results for the energy expectation value. The parameters for these computations were chosen to correspond to Fig. 5 of the Walker-Preston paper ($K = 23.7$, $\mu = 45.11$, $B = 0.0419$), and the agreement with Walker and Preston is excellent. We defer further discussion of such numerical results to Sec. V.

Since the resonance overlap criterion is such a useful tool in the analysis of the classical system, the question arises whether there is a meaningful quantum analogue of resonance overlap. Let us first note that the semiclassical quantization prescription $J \rightarrow (n + \frac{1}{2})\hbar$, which produces the quantum energy levels (4.3) from the classical expression (2.4a), implies that an isolated resonance occurs when

$$\omega_L = N\omega(J_N) = N\omega_0(1 - \omega_0 J_N/2D), \quad (4.10a)$$

$$J_N = (n_N + \frac{1}{2})\hbar. \quad (4.10b)$$

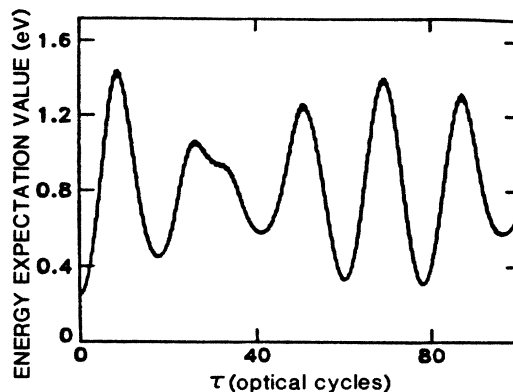


FIG. 6. The energy expectation value for a driven Morse oscillator with parameters $K = 23.7$, $\mu = 45.11$, and $B = 0.0419$. The system is assumed to be in the ground state at $t = 0$. This corresponds to Fig. 5 of the paper by Walker and Preston (Ref. 9).

The width (2.16) then implies

$$\Delta n_N = \frac{2\sqrt{D}}{\hbar\omega_0} \sqrt{|V_N(J_N)|} \quad (4.11)$$

for the number of levels “mixed” by the applied field near an isolated classical N resonance, or equivalently a width

$$\begin{aligned} \Delta E_N &= 2BD[1 - B(n_N + \frac{1}{2})]\Delta n_N \\ &= \hbar\omega_0 \left[1 - \frac{\hbar\omega_0}{2D}(n_N + \frac{1}{2}) \right] \Delta n_N \\ &= \hbar\omega(J_N)\Delta n_N \end{aligned} \quad (4.12)$$

in energy. We now assume a quantum resonance overlap condition of the form

$$\Delta n_{N+1} + \Delta n_N > n_{N+1} - n_N. \quad (4.13)$$

This resonance overlap criterion leads to the same value of the threshold field strength as the classical condition (2.18) when the classical energy E_N is equated to the quantum energy level $E(n_N)$. For a fixed field frequency ω_L , however, there will generally be no quantum energy level for which the classical resonance condition $\omega_L = N\omega(J_N)$ is satisfied exactly.

If the classical nonlinear resonance condition is satisfied for some N , then (4.11) says that the effective “width” in n_N is proportional to $\sqrt{E_0}$, i.e., to the square root of the electric field strength. This Δn_N is a measure of the number of levels near n_N that are strongly coupled, or mixed, by the applied field. The peculiar dependence on E_0 actually appears to have a quantum-mechanical explanation. Consider an $N=1$ classical resonance, $\omega_L = \omega(J_1) \equiv \omega(J_m)$. In quantum terms this resonance condition becomes

$$\begin{aligned} \hbar\omega_L &= (1/2\hbar)[(E_{m+1} - E_m) + (E_m - E_{m-1})] \\ &= BD[2 - 2B(m + \frac{1}{2})]. \end{aligned} \quad (4.14)$$

To see how many levels near m might be strongly coupled by the field in this case, let us consider for simplicity the Schrödinger equation with only nearest-neighbor couplings assumed,

$$\begin{aligned} i\hbar\dot{c}_n &= (E_n - E_m)c_n \\ &\quad - d_1 E_0 (x_{n,n-1}c_{n-1} + x_{n,n+1}c_{n+1})\cos(\omega_L t), \end{aligned} \quad (4.15)$$

where c_n is the probability amplitude for level n and we have measured the energy levels from the level m satisfying (4.14). Now

$$\begin{aligned} E_n - E_m &= BD[2 - 2B(m + \frac{1}{2})](n - m) - B^2D(n - m)^2 \\ &= \hbar\omega_L(n - m) - B^2D(n - m)^2, \end{aligned} \quad (4.16)$$

and so we define C_n by

$$c_n(t) = C_n(t)e^{-in\omega_L t} \quad (4.17)$$

to obtain from (4.15) the equivalent Schrödinger equation

$$\begin{aligned} i\hbar\dot{C}_n &= (E_n - E_m - n\hbar\omega_L)C_n \\ &\quad - d_1 E_0 (x_{n,n-1}C_{n-1}e^{i\omega_L t} + x_{n,n+1}C_{n+1}e^{-i\omega_L t}) \\ &\quad \times \cos(\omega_L t). \end{aligned} \quad (4.18)$$

Under the assumption that the C_n are slowly varying compared with $e^{\pm i\omega_L t}$, we make a rotating-wave approximation,

$$\begin{aligned} i\hbar\dot{C}_n &\cong (E_n - E_m - n\hbar\omega_L)C_n \\ &\quad - \frac{1}{2}d_1 E_0 [x_{n,n-1}C_{n-1} + x_{n,n+1}C_{n+1}] \\ &= -[m\hbar\omega_L + B^2D(n - m)^2]C_n \\ &\quad - \frac{1}{2}d_1 E_0 [x_{n,n-1}C_{n-1} + x_{n,n+1}C_{n+1}]. \end{aligned} \quad (4.19)$$

Now the energy $m\hbar\omega_L$ represents a constant shift and may be removed by redefining the zero of energy. This leaves us with a Schrödinger equation with effective energy levels $\approx (n - m)^2$. We expect strong coupling among those levels “detuned” by an amount comparable to or smaller than the Rabi frequency, which is proportional to E_0 .¹³ This leads us to expect that the spread or “width” of energy levels near m that are strongly coupled by the resonant field is proportional to $\sqrt{E_0}$, as we have inferred above from semiclassical arguments. This point will be discussed further in Sec. VI.

There are different ways in which the dissociation probability may be obtained in our quantum calculations. The most straightforward approach is simply to compute the probability,

$$P_D(t) = \sum_{n=0} |\langle \psi_n | \psi(t) \rangle|^2, \quad (4.20)$$

that the system at any time t is in any one of the 24 bound states. The dissociation probability at time t is then $1 - P_D(t)$. This is the approach taken for the purposes of this paper. For other systems (e.g., the hydrogen atom) this approach may, of course, be impractical.

V. COMPARISON OF CLASSICAL AND QUANTUM THEORIES

As noted in Sec. II, we define the dissociation threshold in the classical calculations by the condition that $\approx 1-3$ trajectories out of 500 reach a compensated energy $E_c > D$ within 90 cycles of the driving field. The dissociation probability at any time t is defined as the fraction of trajectories with $E_c > D$. For some purposes only a few tens of trajectories are needed, but we use typically 500 trajectories for the dissociation calculations in order to obtain smoothly varying dissociation probabilities. In the quantum calculations we similarly define the dissociation threshold to occur when the dissociation probability $1 - P_D$ becomes larger than $1/500$ within 90 cycles.

For “weak” driving fields there is no dissociation. Consider the case when the Morse oscillator starts out in

its ground state and the field frequency is tuned to the $n=0 \rightarrow n=1$ transition ($\mu=45.73$). Figure 7(a) shows the energy expectation value as a function of time. Note that $E_0/D=0.041$ and $E_1/D=0.122$. We do not observe perfectly sinusoidal Rabi oscillations between the $n=0$ and $n=1$ levels because the population does not remain confined to these two levels. Figures 7(b)–7(d)

show the probabilities $|\langle \psi_0 | \psi(t) \rangle|^2$, $|\langle \psi_1 | \psi(t) \rangle|^2$, and $|\langle \psi_2 | \psi(t) \rangle|^2$, respectively, and indicate that most, but not all, of the population resides in the $n=0$ and $n=1$ states. Figure 7(e) shows the expectation value $\langle X(t) \rangle$. In these figures we can discern the rapid field oscillations superposed on the slower Rabi oscillations.

Figures 8(a) and 8(b) show the average energy and in-

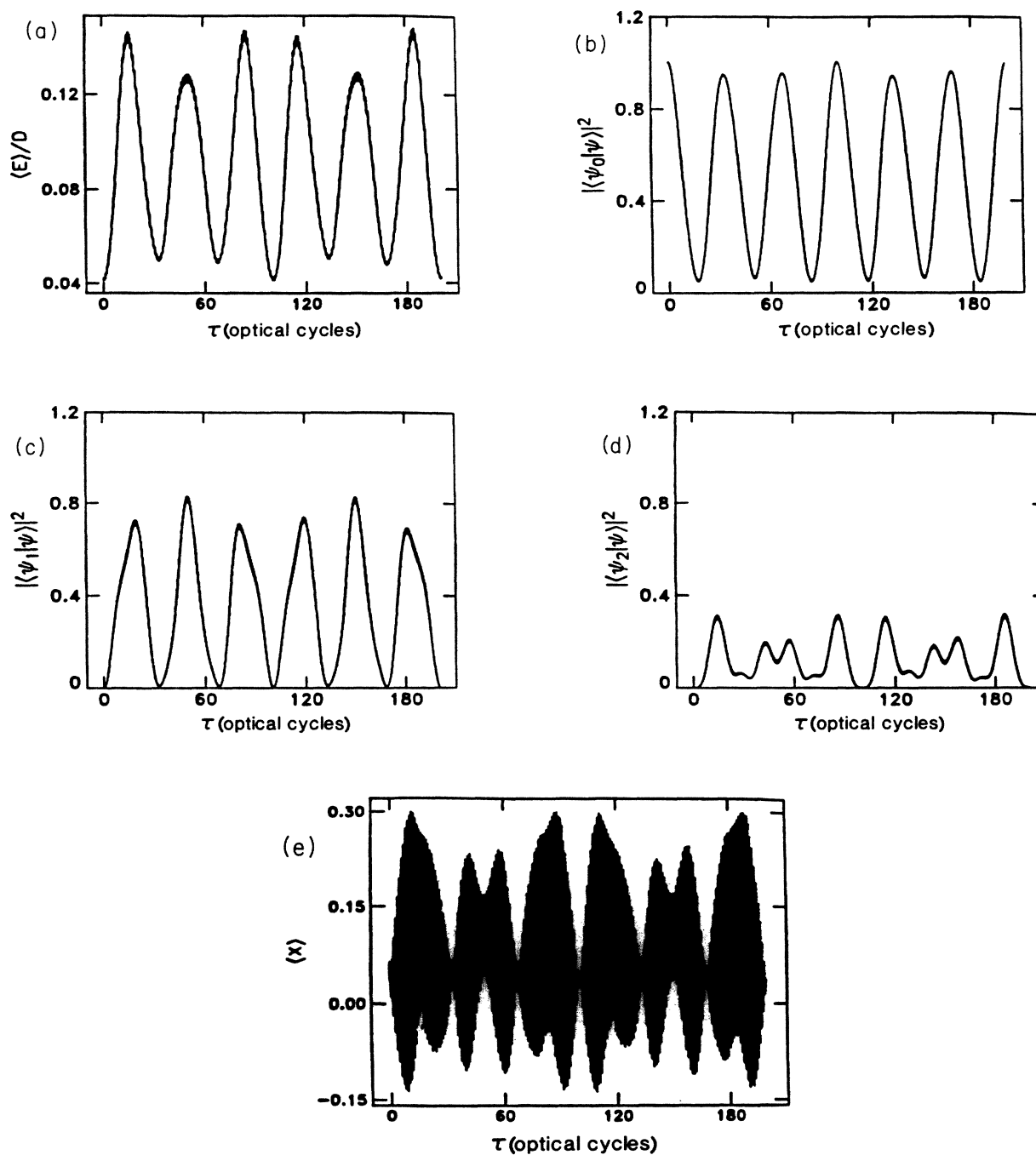


FIG. 7. (a) Energy expectation value for a Morse oscillator with $K=10$, $\mu=45.73$ ($n=0 \rightarrow 1$ resonance), and the initial state $n=0$. (b)–(d) show the probabilities $|\langle \psi_0 | \psi(t) \rangle|^2$, $|\langle \psi_1 | \psi(t) \rangle|^2$, and $|\langle \psi_2 | \psi(t) \rangle|^2$, respectively, and (e) shows the expectation value $\langle X(t) \rangle$ corresponding to the intermolecular separation.

termolecular separation X predicted classically for the case of Fig. 7. For ≈ 10 cycles the classical predictions are in excellent agreement with the quantum results, but for larger times the agreement is not so good. If we use larger values of the driving amplitude the scales of the energy and coordinate variations predicted by the classical and quantum theories are in fairly good agreement, which is consistent with the observations of Walker and Preston.⁹ The good agreement of the classical and quantum predictions for short times could have been anticipated from the energy-time uncertainty relation; for short times the discrete energy levels of the quantum system are "unresolved" and so we have an approximation to the classical continuum of allowed energies. The point that the classical and quantum theories come into better agreement at larger field amplitudes was also made by Shirts and Davis,³ and is discussed further below.

In Fig. 1 we also show the results of quantum calculations (denoted by +) for the threshold field strength for dissociation when the field frequency is set for each initial energy level to the value necessary for a classical $N=1$ resonance. The Morse oscillator is assumed to be

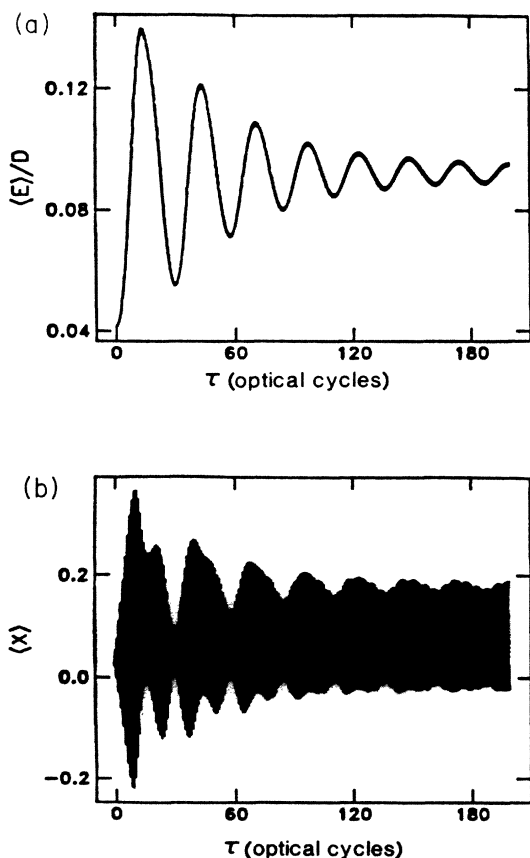


FIG. 8. (a) Average energy and (b) intermolecular separation predicted classically for the case shown in Fig. 7. For short times (≈ 10 cycles) the classical and quantum predictions are in good agreement.

in its ground state before the field is switched on at $t=0$. The agreement with the classical calculations (denoted by \cdot) is rather good at these field strengths required for dissociation, with both the quantum and classical results for K_c being smaller than the value predicted by the simple classical resonance overlap condition. This comparison of the classical and quantum predictions is focused on larger values of E/D in Fig. 2(b) for the $N=1$ resonance, and in Fig. 2(c) for an $N=4$ resonance.

Obviously there is a wide range of parameters that can be investigated. We will simply summarize here what appear to be general trends in the comparison of the classical and quantum theories of the driven Morse oscillator.

(a) The classical and quantum theories are in good agreement for short times, typically ≈ 10 cycles in the parameter range we have focused on. Of course, this result is hardly surprising. For longer times the classical and quantum results look quite different, although the scale of variations is roughly the same.

(b) The simple resonance overlap criterion (2.18) is a fairly accurate predictor of the threshold field strength for dissociation for *both* the classical and quantum theories.

(c) However, the classical and quantum theories can differ substantially near quantum multiphoton resonances *and* near higher-order classical nonlinear resonances, where the resonance frequencies approximate those for single-photon quantum overtone transitions (i.e., $n \rightarrow n+N$, $N > 1$).

The latter point is important for understanding the differences between the classical and quantum theories, and therefore we now discuss it further.

In Fig. 9 we plot the critical value of K for dissociation versus frequency for a Morse oscillator starting in

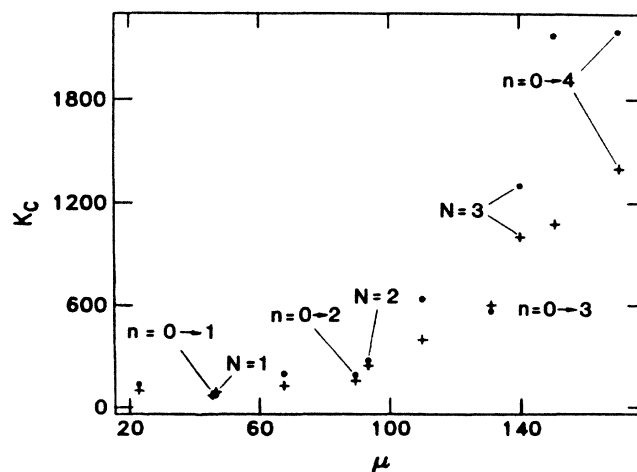


FIG. 9. K_c vs μ for a Morse oscillator starting in the ground state. The labels refer to either an $n=0 \rightarrow N$ quantum overtone resonance or a classical nonlinear N resonance. Unlabeled points do not correspond to a resonance, classical or quantum.

the ground state. It is seen that as we get further from the lower-order resonances the differences between the classical and quantum predictions increase. This is also seen in Fig. 2(c). One way to understand this is as follows. As one goes to higher resonances the resonant frequency for a quantum overtone resonance differs increasingly from the corresponding classical nonlinear resonance. This is shown schematically in Fig. 10. Also indicated are the ranges of frequencies that satisfy the resonance overlap criterion for the various classical resonances. This range is given by

$$\Delta\omega_L = \left| \frac{d\omega_L}{dJ} \right| \Delta J_N = \frac{\omega_0^2}{2D} \Delta J_N. \quad (5.1)$$

Since ΔJ_N decreases with increasing N , $\Delta\omega_L$ decreases as N increases, as seen in Fig. 10. Therefore, as one probes higher overtone resonances the laser frequency gets further outside the classical nonlinear resonance range and consequently a more intense field is typically required for dissociation in the classical system.

It should be emphasized that the agreement between the quantum and classical theories occurs at the low-order resonances and low frequencies. As seen in Fig. 9 the agreement between the quantum and classical theories gets worse, in general, as the frequency is increased. It should also be noted that the agreement discussed here relates to K_c , not the detailed dynamics.

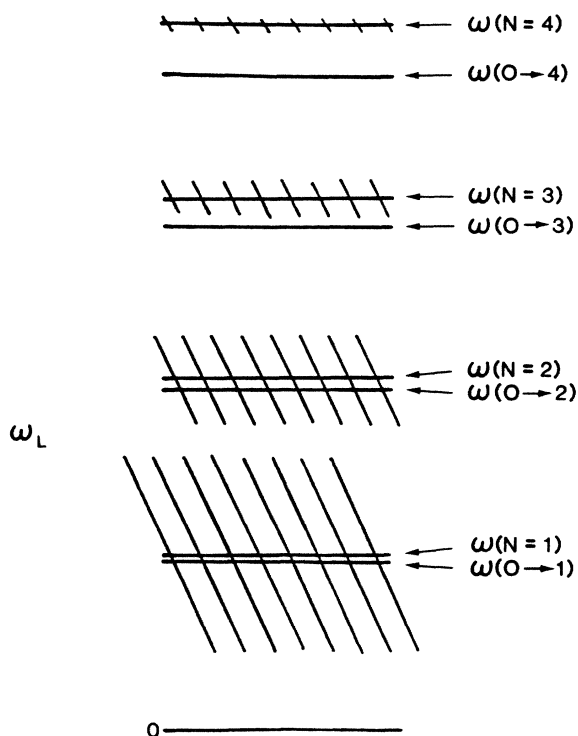


FIG. 10. The laser frequencies for the classical resonances (N) and the corresponding quantum overtone transitions ($0 \rightarrow N$) relative to each other, indicated schematically. The shading indicates the width of the classical resonance for a given value of the field amplitude E_0 .

Mainly we have investigated “experimentally” the regime of rather high field strengths for dissociation. It is perhaps worth emphasizing that even at the lowest-order resonances there can be significant differences between the classical and quantum predictions if the field intensity is weak. This is due again to the fact that the resonance widths scale as the square root of the field amplitude. For weak fields, therefore, the difference between classical and quantum resonance frequencies can lie outside the width of a resonance. An example is shown in Fig. 8, where the average classical energy appears to be decreasing (due to dephasing among different classical trajectories) whereas the quantum expectation value of energy (Fig. 7) is not. As noted above, the possibility of such substantial differences between the classical and quantum predictions at lower field strengths was also recognized by Shirts and Davis.³

VI. CLASSICAL AND QUANTUM CHAOS

Classical chaos may be defined unambiguously by the existence of a positive Lyapunov characteristic exponent, implying the “very sensitive dependence on initial conditions that is the hallmark of chaotic dynamics.”¹⁴ However, the definition of the Lyapunov exponents involves the long-time limit of a system’s dynamics, and for systems like the Morse oscillator the resonance overlap leads to dissociation; we do not know how to characterize the predissociation dynamics as “chaotic” or “regular” in any rigorous fashion. The problem is analogous to that of whether it is meaningful to characterize any *finite* string of digits as random. As noted earlier, Davis and Wyatt² have found that dissociation always appears to occur from “chaotic” regions of phase space in the classical Morse oscillator. By “chaotic” they mean that the surface of section appears to be an erratic sequence of points with no evidence of confinement to KAM (Kolmogorov-Arnold-Moser) tori.

Although we refrain from calling the predissociation dynamics chaotic, it is certainly true that dissociation is preceded by resonance overlap. The question of “quantum chaos” then reduces, for us, to whether there are any quantum-mechanical manifestations of (classical) resonance overlap.

In Sec. IV we deduced from semiclassical considerations that the number of energy levels mixed by a strong field is proportional to the square root of the electric field amplitude. We also offered a heuristic justification of this prediction based on the Schrödinger equation, the rotating-wave approximation, and Rabi splittings (i.e., the so-called “ac Stark effect”¹³). In fact, the prediction

$$\Delta n \propto \sqrt{E_0} \quad (6.1)$$

appears to be confirmed in numerical experiments. Figure 11 shows the probabilities of the Morse oscillator being found in the various bound states for two different values of K with the oscillator starting in the ground state. For $K = 10$ we have ≈ 4 levels significantly populated. For $K = 80$, however, ≈ 11 levels are populated. Figure 12 shows another case, this time with the oscillator starting in the $n = 14$ state. Here we have $\Delta n \approx 6$ for

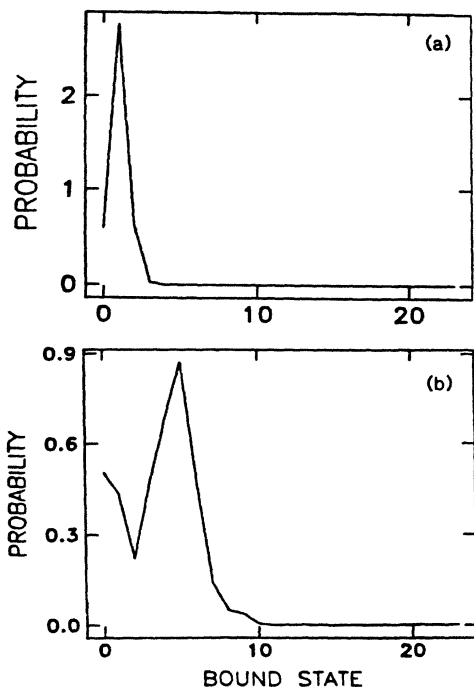


FIG. 11. The probability of being in the various bound states after about 70 optical cycles. The oscillator starts in the ground state with parameters $B=0.0419$ and (a) $K=10.0$, $\mu=45.73$; (b) $K=80.0$, $\mu=45.11$.

$K=2$ and $\Delta n \approx 14$ for $K=15$. In both cases it is seen that the change in Δn with K is in good agreement with (6.1). In our numerical experiments it appeared that the prediction (6.1) was corroborated whenever the spread in Δn was large enough to resolve as in Figs. 11 and 12. Note that *for large field strengths the approximation of purely two-level dynamics breaks down completely*, even at an exact $n \rightarrow n+1$ resonance. Instead of population remaining confined to a "two-level atom," it appears to spread in accordance with (6.1).

It is also worth noting, based on limited numerical evidence available to us, that (6.1) also appears to be supported by quantum calculations for a one-dimensional model of the hydrogen atom in a sinusoidal field.¹⁵ We are presently examining in detail the range of validity of the conjecture (6.1).

Assuming the validity of (6.1), it would appear that classical resonance overlap translates quantum mechanically into a level mixing by the strong field. The number of levels mixed by the field grows with the field strength as $\sqrt{E_0}$, and as E_0 grows the spread of population is enough to give rise eventually to dissociation. The predissociation quantum dynamics is, of course, quasiperiodic, although if enough (discrete) energy levels are mixed by the field the dynamics can be quite complicated.

Such "complicated" but nonchaotic dynamics may suffice in some contexts to justify statistical assumptions about the laser-molecule dynamics. For instance, we recently considered the simple example of a quasiperiodi-

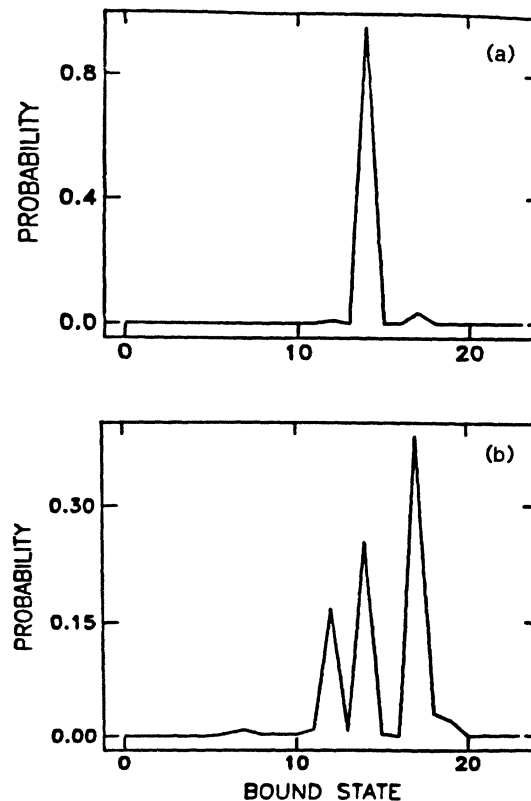


FIG. 12. The probability of being in the various bound states after about 10 optical cycles. The oscillator starts in the $n=14$ state with parameters $\mu=18.67$, $B=0.0419$ and (a) $K=2.0$; (b) $K=15.0$.

cally kicked two-level atom, and found that, although the dynamics is quasiperiodic, it can nevertheless be ergodic on the Bloch sphere; furthermore, the autocorrelation function for the state vector can appear to be a decaying function of the time difference, with recurrences occurring only on long time scales.¹⁶ This nonchaotic behavior is reminiscent of Slater's theory of unimolecular reactions, which invokes a number of incommensurate frequencies to explain certain "statistical" features with purely quasiperiodic dynamics.¹⁷ Similarly, Mazur and Montroll studied ergodic properties of purely harmonic chains using the properties of quasiperiodic functions involving a large number of incommensurate frequencies.¹⁸

As noted earlier, classical models have often been invoked to describe multiple-photon excitation and dissociation. It is typical of recent classical models that dissociation or effectively statistical (incoherent) behavior are consequences of classical resonance overlap^{2,3,6} and chaos.⁶ The mixing of a large number of energy levels by the field may provide a justification for classical dynamics, even though quantum chaos in the strict classical sense of extreme sensitivity to initial conditions may be impossible. In the present example of the driven Morse oscillator, for instance, we have found rather good agreement between the classical and quantum pre-

dictions for the dissociation threshold, except near higher-order classical and quantum resonances.

Note added in proof. Questions of resonance overlap and localization in the driven Morse oscillator have also been addressed in a brief note by H ohnerbach and Graham.¹⁹ These authors define a classical diffusion constant and a mean first passage time for diffusion across the dissociation border, which they indicate to be in good qualitative agreement with numerical (classical) results.

ACKNOWLEDGMENTS

This work was supported in part by National Science Foundation Grant No. PHY-8418070 at the University of Arkansas. We thank Dr. J. R. Ackerhalt for useful discussions related to this work. Some helpful remarks by M. M. Sanders and Dr. R. B. Walker are also gratefully acknowledged. Finally, we thank Dr. R. Shirts and other participants in the 1987 Telluride Workshop on Laser-Molecule Interactions for sharing their insights about such problems.

-
- ¹See, for instance, G. Herzberg, *Spectra of Diatomic Molecules* (Van Nostrand, Princeton, 1964), p. 101.
- ²M. J. Davis and R. E. Wyatt, *Chem. Phys. Lett.* **86**, 235 (1982).
- ³R. M. O. Galvao, L. C. M. Miranda, and J. T. Mendonca, *J. Phys. B* **17**, L577 (1984); also see R. B. Shirts and T. F. Davis, *J. Phys. Chem.* **88**, 4665 (1984).
- ⁴B. V. Chirikov, *Phys. Rep.* **52**, 263 (1979).
- ⁵E. V. Shuryak, *Zh. Eksp. Teor. Phys.* **71**, 2039 (1976) [*Sov. Phys.—JETP* **44**, 1070 (1976)].
- ⁶See, for instance, D. A. Jones and I. C. Percival, *J. Phys. B* **12**, 709 (1979); J. R. Ackerhalt and P. W. Milonni, *Phys. Rev. A* **34**, 1211 (1986); **34**, 5137 (1986) (E).
- ⁷D. R. Grempel, R. E. Prange, and S. Fishman, *Phys. Rev. A* **29**, 1639 (1984).
- ⁸See, for instance, N. Bloembergen, *Opt. Commun.* **15**, 416 (1975); W. E. Lamb, Jr., in *Laser Spectroscopy III*, edited by J. L. Hall and J. L. Carlsten (Springer-Verlag, New York, 1977) and *Laser Spectroscopy IV*, edited by H. Walther and K. Rothe (Springer-Verlag, New York, 1979).
- ⁹R. B. Walker and R. K. Preston, *J. Chem. Phys.* **67**, 2017 (1977).
- ¹⁰J. G. Leopold and I. C. Percival, *Phys. Rev. Lett.* **41**, 944 (1978).
- ¹¹P. M. Morse, *Phys. Rev.* **34**, 57 (1929); D. ter Haar, *Phys. Rev.* **70**, 222 (1946).
- ¹²R. D. Richtmyer, *Difference Methods for Initial-Value Problems* (Interscience, New York, 1957); S. E. Koonin, *Computational Physics* (Benjamin/Cummings, Menlo Park, CA, 1986).
- ¹³For a review of Rabi splitting effects see, for instance, P. L. Knight and P. W. Milonni, *Phys. Rep.* **66**, 21 (1980).
- ¹⁴An introduction to the subject is given by P. W. Milonni, M.-L. Shih, and J. R. Ackerhalt, *Chaos in Laser-Matter Interactions* (World Scientific, Singapore, 1987).
- ¹⁵M. M. Sanders (private communication).
- ¹⁶P. W. Milonni, J. R. Ackerhalt, and M. E. Goggin, *Phys. Rev. A* **35**, 1714 (1987).
- ¹⁷N. B. Slater, *Theory of Unimolecular Reactions* (Cornell University Press, Ithaca, 1959).
- ¹⁸P. Mazur and E. Montroll, *J. Math. Phys.* **1**, 70 (1960).
- ¹⁹R. H ohnerbach and R. Graham, in *Fundamentals of Quantum Optics II*, edited by F. Ehlotzky (Springer, New York, 1987).

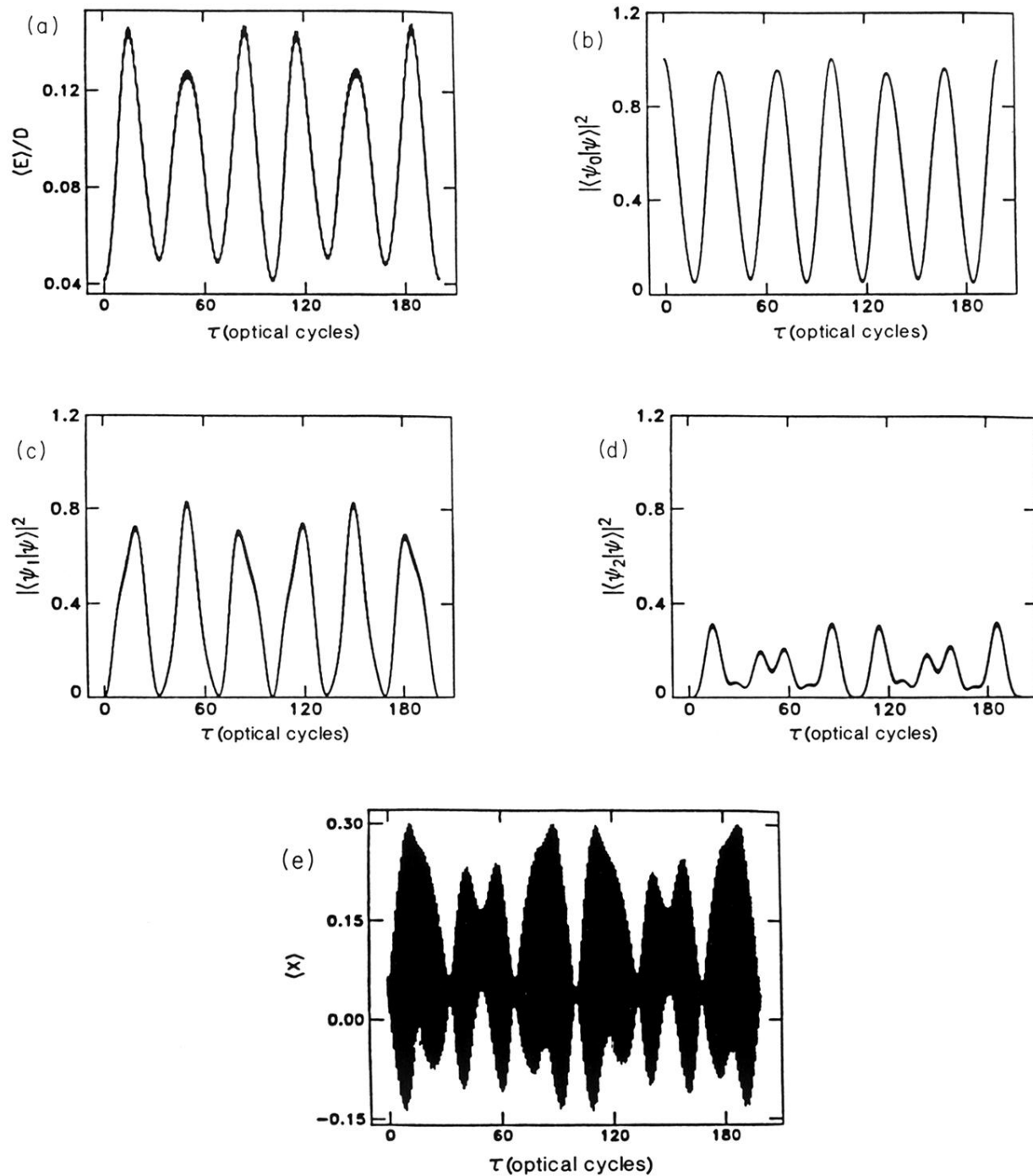


FIG. 7. (a) Energy expectation value for a Morse oscillator with $K = 10$, $\mu = 45.73$ ($n = 0 \rightarrow 1$ resonance), and the initial state $n = 0$. (b)–(d) show the probabilities $|\langle \psi_0 | \psi(t) \rangle|^2$, $|\langle \psi_1 | \psi(t) \rangle|^2$, and $|\langle \psi_2 | \psi(t) \rangle|^2$, respectively, and (e) shows the expectation value $\langle X(t) \rangle$ corresponding to the intermolecular separation.

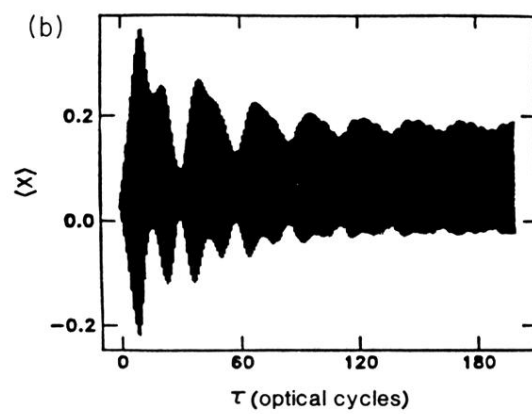
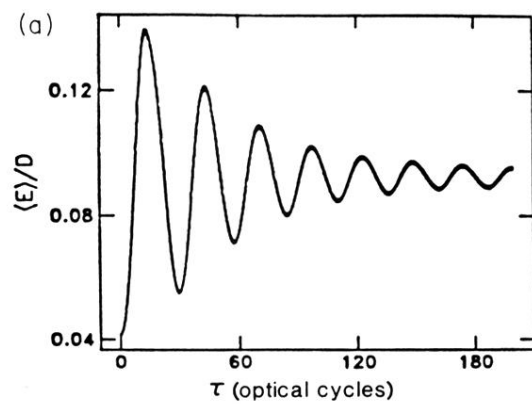


FIG. 8. (a) Average energy and (b) intermolecular separation predicted classically for the case shown in Fig. 7. For short times (≈ 10 cycles) the classical and quantum predictions are in good agreement.